

GA-A27419

LONG-PULSE STABILITY LIMITS OF ITER BASELINE SCENARIO PLASMAS IN DIII-D

by

G.L. JACKSON, F. TURCO, T.C. LUCE, R.J. BUTTERY, A.W. HYATT, J.S. DEGRASSIE,
E.J. DOYLE, J.R. FERRON, R.J. LA HAYE, R. NAZIKIAN, P.A. POLITZER, W.M. SOLOMON
and M.R. WADE

OCTOBER 2012



DISCLAIMER

This report was prepared as an account of work sponsored by an agency of the United States Government. Neither the United States Government nor any agency thereof, nor any of their employees, makes any warranty, express or implied, or assumes any legal liability or responsibility for the accuracy, completeness, or usefulness of any information, apparatus, product, or process disclosed, or represents that its use would not infringe privately owned rights. Reference herein to any specific commercial product, process, or service by trade name, trademark, manufacturer, or otherwise, does not necessarily constitute or imply its endorsement, recommendation, or favoring by the United States Government or any agency thereof. The views and opinions of authors expressed herein do not necessarily state or reflect those of the United States Government or any agency thereof.

LONG-PULSE STABILITY LIMITS OF ITER BASELINE SCENARIO PLASMAS IN DIII-D

by

G.L. JACKSON¹, F. TURCO³, T.C. LUCE¹, R.J. BUTTERY¹, A.W. HYATT¹,
J.S. DEGRASSIE¹, E.J. DOYLE⁴, J.R. FERRON¹, R.J. LA HAYE¹, R. NAZIKIAN²,
P.A. POLITZER¹, W.M. SOLOMON² and M.R. WADE¹

This is a preprint of a paper to be presented at the Twenty-fourth
IAEA Fusion Energy Conf., October 8-13, 2012 in San Diego,
California.

¹General Atomics, P.O. Box 85608, San Diego, California.

²Princeton Plasma Physics Laboratory, Princeton, New Jersey.

³Columbia University, New York, New York.

⁴University of California Los Angeles, Los Angeles, California.

Work supported in part by
the U.S. Department of Energy
under DE-FC02-04ER54698, DE-AC02-09CH11466, DE-FG02-04ER54761,
and DE-FG02-08ER54984

GENERAL ATOMICS PROJECT 30200
OCTOBER 2012

Long-Pulse Stability Limits of ITER Baseline Scenario

G.L. Jackson¹, F. Turco³, T.C. Luce¹, R.J. Buttery¹, A.W. Hyatt¹, J.S. deGrassie¹, E.J. Doyle⁴, J.R. Ferron¹, R.J. La Haye¹, R. Nazikian², P.A. Politzer¹, W.M. Solomon², and M.R. Wade¹

¹General Atomics, P.O. Box 85608, San Diego, California 92186-5608, USA

²Princeton Plasma Physics Laboratory, Princeton, New Jersey 08543-0451, USA

³Columbia University, New York, New York 10027, USA

⁴University of California Los Angeles, Los Angeles, California 90095-7099

Abstract. Long duration plasmas, stable to $m/n=2/1$ tearing modes (TMs), with an ITER similar shape and I_p/aB_T , have been demonstrated in DIII-D, evolving to stationary conditions with the most stable operating region, $\beta_N \approx 1.8-2$. The stability range for these ITER baseline scenario (IBS) pulses has been observed over a range of peak initial internal inductance, $0.9 \leq l_{i,start} \leq 1.25$. Low applied external torque, at or below the extrapolated value expected for ITER has also been demonstrated. With electron cyclotron current drive, the region of stable discharges has been further extended, including ELM free discharges using the DIII-D internal coil set. In addition, dominant electron heating in the ITER shape has been demonstrated

1. Introduction

Long duration plasmas, stable to $m/n=2/1$ tearing modes (TMs), with an ITER similar shape and I_p/aB_T , have been demonstrated in DIII-D, evolving to stationary conditions, with the most stable operating region found to be $\beta_N \approx 1.8-2$. The goal of these experiments was to simulate ITER conditions as closely as possible, scaling ITER parameters to the DIII-D tokamak. Previous ITER baseline scenario (IBS) experiments [1,2] have focused on developing an ITER similar shape in DIII-D, demonstrating current rampup within the ITER constraints, and in obtaining successful rampdown including an H-L back transition while holding the outer strikepoint fixed. In the experiments reported here we have explored the access region for long pulse stable discharge and reduced NB torque to ITER relevant values, without electron cyclotron current drive (ECCD). ECCD has been used for TM stabilization at reduced density, allowing stable edge localized mode (ELM)-free operation with an $n=3$ perturbative field. In addition, electron cyclotron heating (ECH) has demonstrated pulses with dominant electron heating.

Initial exploration of a stable IBS operating regime in the 2011 campaign found best results for $\beta_N \approx 2$. In these discharges, the outer strike point was not positioned to effectively utilize the outer cryopump, sometimes even positioned on the “nose” of the pumping baffle [Fig. 1(c), green trace]. A small shift to higher triangularity in the 2012 campaign, [Fig. 1(c), blue], produced more effective pumping and a larger stability region, discussed in Sec. 2.

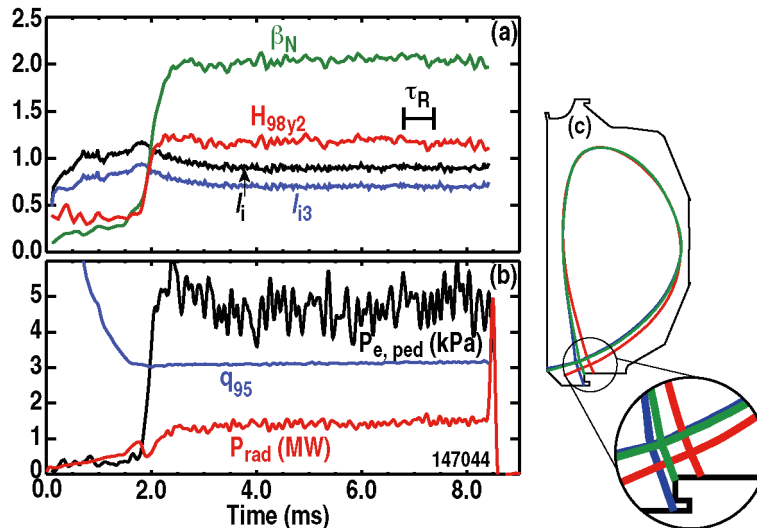


Fig. 1. Pulse with an ITER baseline shape without ECCD and nearly stationary parameters, (a) β_N (green), H_{98y2} (red), l_i (black), and l_3 (blue); (b) electron pedestal pressure (black), total radiated power (red) and q_{95} (blue). ITER scaled shape and the DIII-D approximation are shown in (c). blue, 2012 campaign, green, 2011 campaign, red scaled ITER shape. ITER/DIII-D scale factor = 3.59. Plasma parameters are: $I_p/aB_T = 1.40$, co-NBI ≈ 3.0 MW.

The addition of ECCD produced stable operation in plasmas which were otherwise found to be unstable (usually at low density) and allowed suppression of ELMs at the ITER similar value of $q_{95} = 3.19$ and $I_p/aB_T = 1.41$, utilizing a single toroidal row of internal coils (I-coils).

In this paper we refer to the ITER baseline scenario, or IBS, as pulses having an ITER shape scaled to DIII-D [2] and, except for the dominant electron heating pulses, also having approximately the same normalized plasma current as the 15 MA ITER baseline scenario, namely $I_p/aB_T = 1.415$.

The paper is organized as follows: Sections 2 and 3 present experiments to explore the regions of stability for long pulse operation without using ECCD for $m/n=2/1$ mitigation including pulses at ITER relevant values of torque. Section 4 discusses operation with ECCD or ECH leading to stable operation at lower density, followed by conclusions in Sec. 5.

2. Limits to Stable Operation in Long Duration Pulses

Long pulse plasmas ($\Delta t_{\text{duration}} \leq 7.5$ s and $\leq 11\tau_R$), without ECCD for TM mitigation, have extended shorter pulse experiments in which the internal inductance, l_i , was continually evolving [3]. Without ECCD TMs or locked modes often occurred which would degrade or

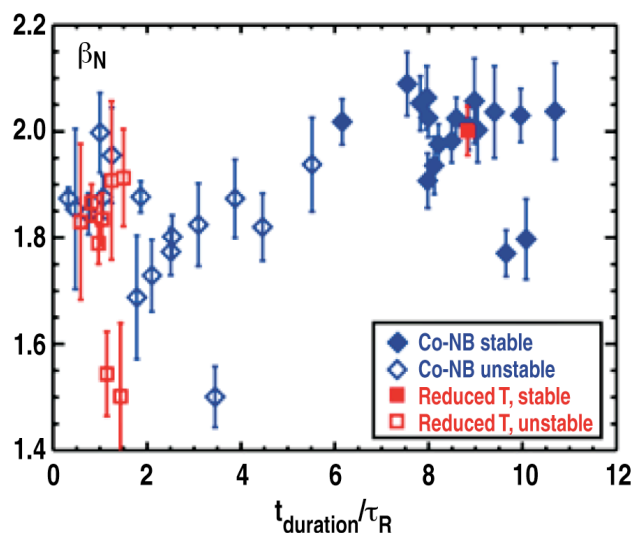


Fig. 2. Time averaged β_N as a function of duration of the flattop phase t_{duration} normalized to the resistive time τ_R for the 2011 campaign. Red symbols denote plasmas with a fraction of counter- I_p NBI and blue symbols denote only co- I_p NBI. All cases shown are without ECCD.

terminate the discharge. Without ECCD, near-stationary conditions have been achieved, stable against TMs, e.g. Fig. 1, demonstrating that access to steady state ITER baseline scenario is possible. However in some cases with similar programming, $m/n=2/1$ tearing modes and locked modes limited the duration, indicating operation near stability limits. This was particularly evident as β_N was reduced in the 2011 IBS campaign, shown in Fig. 2. For example, 84% of plasmas were stable to 2/1 TMs with neutral beam injection (NBI) only in the co- I_p direction for $1.9 \leq \beta_N \leq 2.1$ (Fig. 2), but only 15% were stable in the ITER baseline scenario range, $1.7 \leq \beta_N \leq 1.9$.

A second campaign to explore a broader stability region was carried out in 2012. In this 2012 campaign, the outer divertor strike point was positioned closer to optimal pumping, the initial density programming was changed for better control in the current rise, careful attention was paid to the discharge termination (which can affect the next pulse), and $n_{e,\text{flattop}}$ was higher. As shown in Fig. 3, a higher fraction of stable discharges were achieved (blue triangles), although operation was generally at a higher average density. The ordinate in Fig. 3 is the average normalized current density, $j_{95N,\text{av}}$ during the β_N flattop phase, where j_{95N} is the flux surface average toroidal current density at 95% of normalized poloidal flux normalized to I_p/A_{plasma} and A_{plasma} is the cross-sectional plasma area.

During part of the 2012 IBS campaign, many discharges exhibited a radiative collapse due to an influx of metal impurities. These impurities arose from previous experiments where arcing of the fast wave antennas deposited metals on other plasma facing surfaces (this was subsequently repaired). The radiative collapses occurred without $m/n=2/1$ TM activity i.e., the discharges were TM stable up to the time of the radiative collapse and thus are considered as stable points in Fig. 3. We also note in Fig. 3 that pedestal current density, $j_{95N,\text{av}}$, increases as electron density decreases for stable discharges above an apparent threshold, $n_{e,\text{flattop}} > 5.2 \times 10^{19} \text{ m}^{-3}$. Thus there is a stable operating region, $n_{e,\text{flattop}} > 5.2 \times 10^{19} \text{ m}^{-3}$ for the discharge conditions in Fig. 3 ($B_T = 1.6 \text{ T}$ and $1.38 \leq I_p/aB_T \leq 1.42$).

The correlation of $j_{95N,\text{av}}$ to 2/1 TM stability is summarized in Fig. 4 for an expanded set of data including all pulses from the 2011 and 2012 IBS campaigns (including low torque pulses discussed below) but without ECCD, radiative collapse, or early NB heating. Although there is overlap in $j_{95N,\text{av}}$ between stable and unstable pulses, best stability is generally observed at higher $j_{95N,\text{av}}$, i.e. greater than 0.47. In Fig. 4, 91% of the stable pulses were obtained with $j_{95N,\text{av}} \geq 0.47$ while 74% of the unstable pulses had $j_{95N,\text{av}} < 0.47$. We note that planned IBS operation is at $\beta_N=1.8$. At this value reliable operation in DIII-D without ECCD

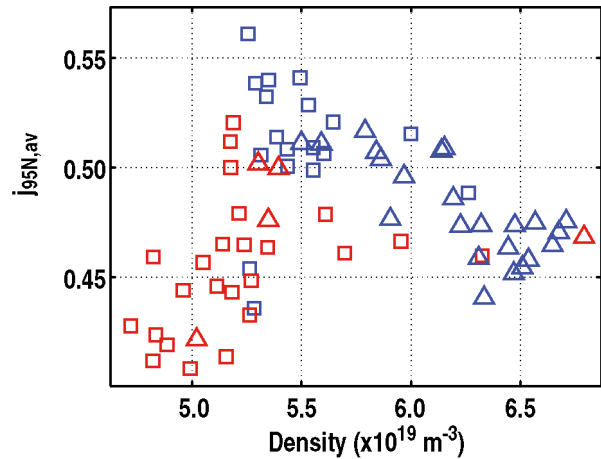


Fig. 3. Comparison of discharges at $B_T=1.6 \text{ T}$ for the 2011 (squares) and 2012 (triangles) IBS campaigns. Pulses with a β_N collapse due to $m/n=2/1$ TMs are plotted in red. All discharges are with co-NBI and without ECCD.

was obtained (blue triangles), but only after improvements in operating conditions described previously, indicating that these discharges were near TM stability limits.

With the changes described above for the 2012 IBS campaign, the I_p ramp rate was varied to change the initial internal inductance, $l_{i,start}$, leading to an expanded region for stable IBS discharges compared to the 2011 campaign, shown in Fig. 5. This range of $l_{i,start}$ can simulate conditions which are accessible in proposed ITER scenarios. The goal was to explore whether different l_i (and hence different current profiles) might lead to conditions of stable flat-top plasmas. In this scan, discharges stable to $m/n=2/1$ TMs (including those with radiative collapses) were demonstrated over the range of internal inductance scanned, $0.9 \leq l_{i,start} \leq 1.25$. For the conditions of the 2012 campaign, the initial value of internal inductance, $l_{i,start}$, at the beginning of the β_N flat-top phase had little effect on stability to 2/1 TMs for $1.7 \leq \beta_N \leq 2.1$.

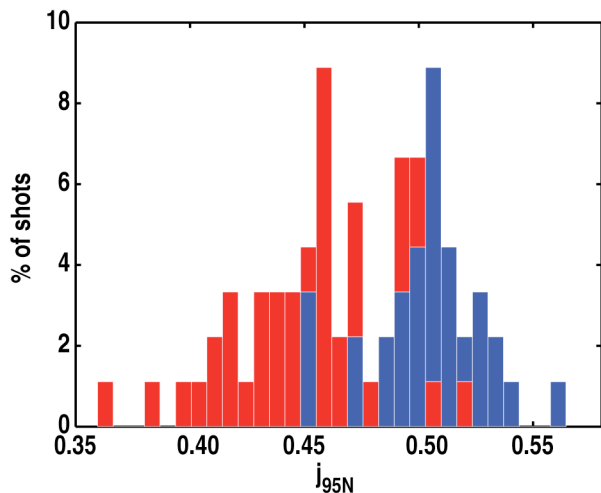


Fig. 4. Histogram of normalized current density (averaged over the β_N flat-top phase) at $\psi_N = 0.95$ for stable (blue) and unstable (red) discharges from both the 2011 and 2012 campaigns. $B_T = 1.6-1.8$ T and $I_p/aB_T = 1.38-1.42$. Pulses with ECCD, early NB heating, or a radiative collapse are excluded from this data set.

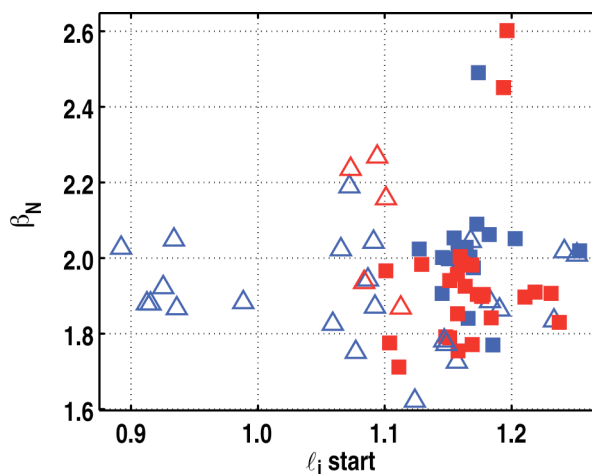


Fig. 5. Stability region for IBS discharges. Stable discharges, up to programmed current rampdown or radiative collapse, are shown in blue. Red points are unstable. Triangles are from the 2012 IBS campaign, squares are from the 2011. Discharges are co-NB injection, $B_T = 1.6$ T and $I_p/aB_T = 1.38-1.42$.

3. Stability at Low Torque

In order to better simulate ITER conditions, neutral beam driven torque was reduced from full co-injection, $\approx 2-3$ N-m (Fig. 6). Stable operation without ECCD was achieved at or below the estimated ITER torque range [4]. As the torque was reduced, the stable region of

dI_p/dt and $\ell_{i,start}$ was also reduced, as shown in Fig. 6. Although not shown explicitly in Fig. 4, all of the stable low torque pulses ($T < 1$ Nm in Fig. 6) had $j_{95N,av} \geq 0.50$ and there was no significant change in $j_{95N,av}$ as the torque was scanned from 2.5 Nm to 0.36 Nm for the stable discharges. Electron density was not varied appreciably during this torque scan and was well above the threshold observed in Fig. 3, hence any density dependence at reduced torque requires additional experiments. For NB torques at or below 0.36 N-m, the discharges were unstable to TMs. However a stable operating range does exist within the range of the estimated ITER extrapolated torque (vertical line in Fig. 6). Using the fit to the data in [Fig. 6(c)], normalized confinement, H_{89P} is lower in this torque scan by 15% when torque is reduced from 2.5 to 0.36 N-m.

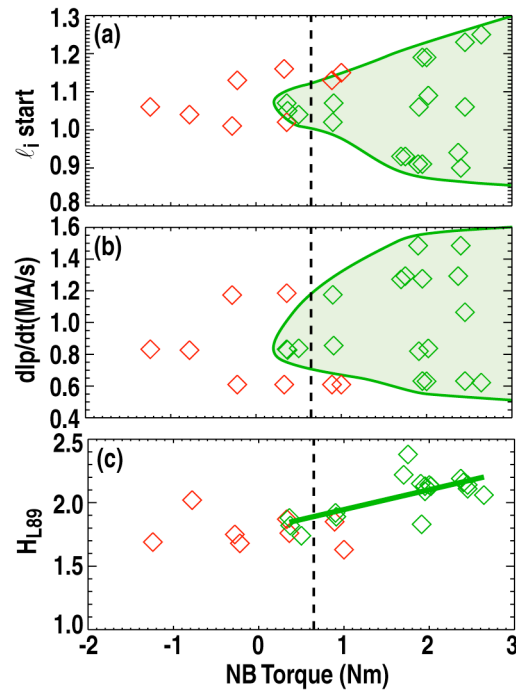


Fig. 6. Torque scan for ITER baseline discharges with unstable (red) and MHD stable (green) discharges. Initial value of internal inductance, (a) was varied by changing the I_p ramp rate, (b). Normalized confinement, H_{89P} , is plotted in (c). A first order polynomial fit for stable discharges is plotted in (c), green line and the vertical dashed line indicates the approximate ITER torque, scaled to DIII-D [4]. $B_T = 1.8$ T, $I_p/aB_T = 1.40-1.42$.

4. EC for Enhanced Stability and Dominant Electron Heating

To mitigate 2/1 TMs, especially at lower density, ECCD was applied. Broad ECCD deposition was found to be most effective when positioned near the $q=3/2$ flux surface plotted in Fig. 7(a). In contrast, ECCD deposition further out (black traces, Fig. 7) led to prompt locked modes, at least for the limited database in these experiments. For the discharges in Fig. 7, the temporal evolution (including j_{95N}) was similar until counter beams were applied to reduce the torque to more ITER relevant conditions. With reduced toroidal rotation [Fig. 7(c)], the plasma with ECCD near $q=3/2$ was sustained nearly to the time of

programmed I_p rampdown [Fig. 7(d)] while the other discharge developed a locked mode almost immediately after the torque was reduced. In both cases, the locked mode occurred within 0.1 s after the toroidal rotation dropped to zero. We note that narrow ECCD deposition at $q=2$ and active tracking were not attempted in these experiments nor was sawtooth mitigation possible [5] due to geometrical limitations in aiming the ECCD inside the sawtooth inversion radius for the pulses in Fig. 7 at $B_T = 1.6$ T.

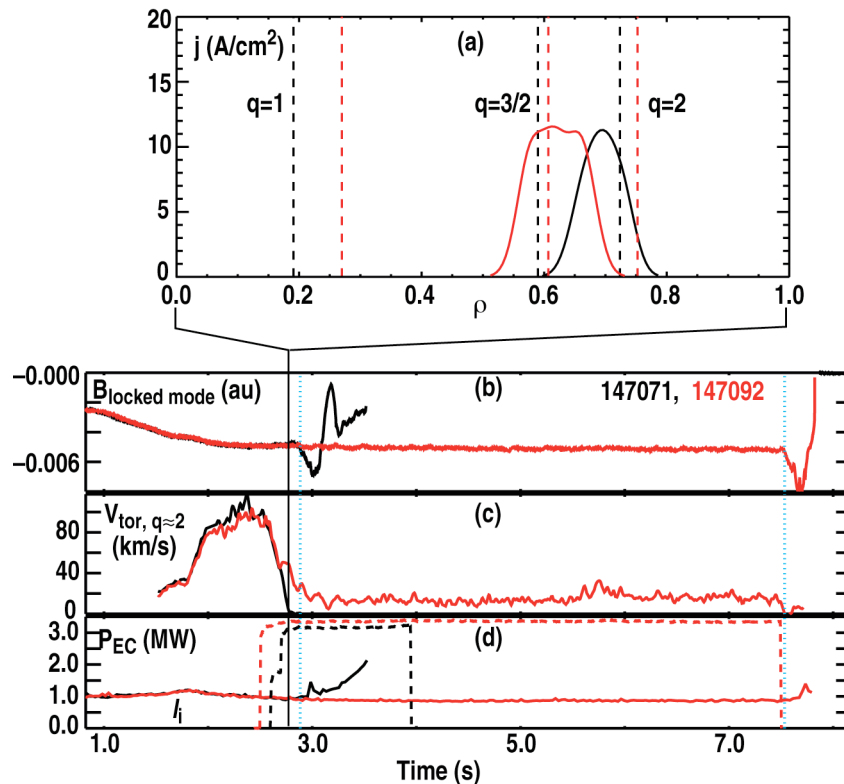


Fig. 7. (a) ECCD current density at two locations, (b) $n=1$ locked mode detector, (c) toroidal velocity near the $q=2$ flux surface, and (d) EC power (dashed) and I_i . Discharge evolution was similar until $t = 2.5$ s when counter torque was applied. $\beta_N = 2.0$ and $T_{max} = 2.7$ Nm. In the sustained discharge (red), $T_{flatop} = 1.2$ Nm, $n_e = 4.6 \times 10^{19} \text{ m}^{-3}$, $j_{95N,av} = 0.55$. Dotted vertical lines (blue) show locked mode onset.

The application of ECCD allowed stable plasmas at lower densities, characteristic of density pumpout when a 3-D perturbative magnetic field was applied, Fig. 8. With this $n=3$ non-axisymmetric magnetic field, produced by the upper row of the internal coil set (I-coils) ELM suppression was achieved Fig. 8. These plasmas ($I_p/aB_T = 1.41$, $q_{95} = 3.19$, and co- I_p NBI) were obtained for durations up to 3.5 s with only the upper row of six I-coils, providing a broad $n=3$ spectrum [6]. Confinement [Fig. 8(d)] was lower with ECCD and the I-coils, but it was sensitive to the ECCD power and actually increased near the end of the pulse as EC power was reduced while the discharge remained stable. Future work will explore stable regimes with ELM suppression at higher confinement.

EC heating has also been used to achieve dominant electron heating in an IBS shape. Presently, pulses with $P_{NB} = 1$ MW and $P_{ECH} = 2.8$ MW have been achieved with β_N up to

1.8 and $q_{95} = 4.2$. Future work will explore this regime at the IBS value of $I_p/aB_T = 1.415$, $q_{95} \approx 3.1$.

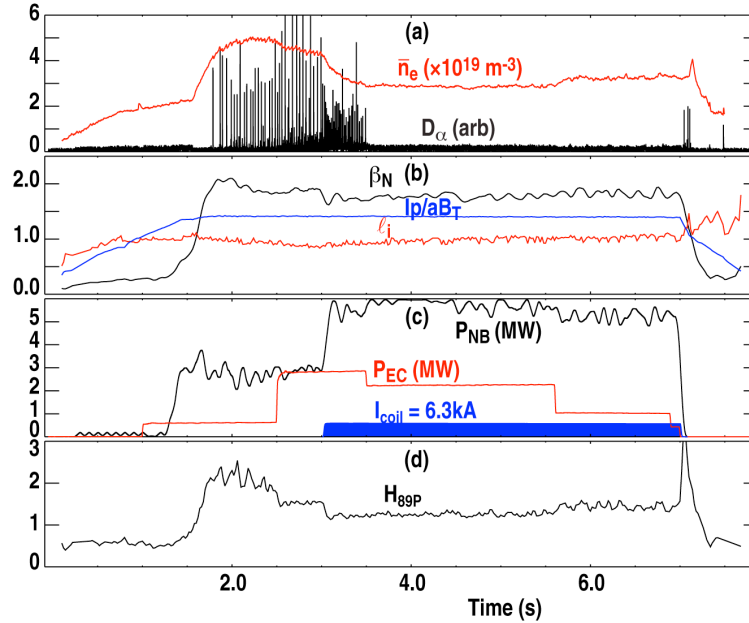


Fig. 8. ELM suppression with the upper row of 3-D I-coils; (a) divertor D_α and electron density, (b) β_N , normalized current, and internal inductance, (c) neutral beam and EC power, and (d) normalized confinement factor, H_{89P} .

5. Discussion and Summary

There has been steady progress in demonstrating conditions required for ITER baseline scenario operation. Stationary plasmas in an ITER similar shape stable to 2/1 tearing modes have successfully been obtained for up to $\approx 11 \tau_R$ under a variety of conditions, with most reliable operation at $\beta_N \approx 1.8$ –2. By varying the I_p ramp rate, pulses stable to $m/n=2/1$ tearing modes have been demonstrated from $0.9 \leq l_{i,start} \leq 1.25$ and with low torque operation in a range simulating the expected ITER torque. This extends previous work [3] with shorter pulses in which plasmas evolved until the onset of TMs. For these pulses, without ECCD, a density threshold was observed below which nearly all pulses exhibited 2/1 TMs. In addition, a correlation between pedestal current density, $j_{95N,av}$ and long duration stable pulses have been observed in this dataset, discussed later.

The addition of EC heating or ECCD near the $q=3/2$ surface allowed stability at lower density than obtained with NB heating only (Sec. 2), leading to pulses with no ELMs (using the DIII-D internal 3-D coil set) and also to a demonstration of dominant electron heating, as envisaged for ITER.

In these studies, we have observed a correlation between density and normalized pedestal current, $j_{95N,av}$ and an apparent density limit (at constant B_T , q_{95} , and without EC stabilization) below which $m/n=2/1$ TMs terminate the β_N flattop phase. For these ITER baseline scenario (IBS) discharges at fixed B_T , co-NB heating, and $I_p/aB_T = 1.38$ –1.42, this limit was $5.2 \times 10^{19} \text{ m}^{-3}$. The relationship between $j_{95N,av}$ and the onset of the 2/1TMs is under

investigation; at present it is simply an empirical observation and needs to be validated with further experiments. Our working hypothesis is that higher pedestal current density may be an indication of a lower current density gradient at the 2/1 surface, which is stabilizing to these modes. However the DIII-D diagnostic set does not have sufficient resolution to test this hypothesis at present. If $j_{95N,av}$ is indeed a sensitive parameter to 2/1 TM stability, external control of this parameter would be very useful. We have not found a strong correlation between $j_{95N,av}$ and the initial internal inductance, $l_{i,start}$. As presented in Sec. 2, the most stable operation occurs above an electron density threshold and this is usually accompanied by $j_{95N,av}$ also above a threshold. Future work will investigate the relationship between electron density and $j_{95N,av}$. Planned operation for ITER is with electron density at a high fraction of the Greenwald density limit. The density limit found in this work, $5.2 \times 10^{19} \text{ m}^{-3}$, corresponds to $n_e/n_{GW} = 0.42$ which should provide a sufficient operating range for ITER.

The sensitivity to small changes in discharge conditions between the 2011 and 2012 campaigns indicates operation near the stability region for these IBS discharges. Small improvements to the mode of operation, discussed in Sec. 2, led to improved stability in the 2012 campaign. No single parameter showed a significant difference between these two campaigns. For example Z_{eff} (primarily due to carbon), which might be expected to be lower in the 2012 campaign, did not show a consistent correlation. As noted above however, without EC heating or current drive, there appears to be a threshold in density, $n_e \approx 5.2 \times 10^{19} \text{ m}^{-3}$ for the experimental conditions in Fig. 3, below which 2/1 TMs are more prevalent. The dependence of this threshold on parameters such as β_N , B_T , and q_{95} , remains to be investigated.

Although we have demonstrated nearly all elements of an ITER baseline discharge in separate pulses, future work will aim at providing a complete ITER demonstration in a single pulse; i.e., stable operation in the ITER shape with $I_p/aB = 1.415$, $\beta_N = 1.8$, an ITER relevant torque, with either no or small ELMs acceptable for ITER operation, and dominant electron heating.

This work was supported by the US Department of Energy under DE-FC02-04ER54698, DE-AC02-09CH11466, DE-FG02-04ER54761, and DE-FG02-08ER54984.

References

- [1] DOYLE, E.J. et al. Nucl. Fusion **50** (2010) 075005
- [2] JACKSON, G.L. et al. Phys. Plasma **17** (2010) 056116
- [3] TURCO, F. and LUCE, T.C. Nucl. Fusion **50** (2010) 095010
- [4] GARAFALO, A.G. et al. Nucl. Fusion **51** (2011) 083018
- [5] CHAPMAN, I.T. et al. Nucl. Fusion **52** (2012) 063006
- [6] DEGRASSIE, J.S. et al. "Suppression of ELMs by Resonant Magnetic Perturbations in DIII-D in the ITER Similar Shape," submitted to Nucl. Fusion, 2012